Interlesional Heterogeneity of Metastatic Neuroendocrine Tumors Based on 18F-DOPA PET/CT

de Hosson, Lotte D.; van der Loo-van der Schaaf, Aline M.; Boellaard, Ronald; van Snick, Johannes H.; de Vries, Elisabeth G. E.; Brouwers, Adrienne H.; Walenkamp, Annemiek M. E.

Published in:
Clinical Nuclear Medicine

DOI:
10.1097/RLU.0000000000002640

Document Version
Publisher's PDF, also known as Version of record

Publication date:
2019

Interlesional Heterogeneity of Metastatic Neuroendocrine Tumors Based on ^{18}F-DOPA PET/CT

Lotte D. de Hosson, MD, PhD, Aline M. van der Loo–van der Schaaf, MD,† Ronald Boellaard, PhD,‡ Johannes H. van Snick,‡ Elisabeth G. E. de Vries, MD, PhD,* Adrienne H. Brouwers, MD, PhD,‡ and Annemiek M. E. Walenkamp, MD, PhD**

Purpose: Neuroendocrine tumors (NETs) can produce neuroendocrine amines resulting in symptoms. Selecting the most active amine-producing tumor lesions for local treatment might be beneficial for patients with metastatic small intestinal NET. Tumor burden correlates with catecholamine pathway activity. We analyzed interlesional heterogeneity with ^{18}F-DOPA PET scans in patients with small intestinal NET and investigated if lesions with substantially higher ^{18}F-DOPA uptake could be identified.

Methods: In this retrospective, observational study, the ^{18}F-DOPA uptake was calculated by dividing SUVpeak of the lesion by the SUVmean of the background organ. The magnitude of heterogeneity between lesions within a patient was calculated by dividing the lesion with the highest by the one with the lowest ^{18}F-DOPA uptake. Lesions with a higher ^{18}F-DOPA uptake than the upper inner or outer fence (>1.5 or 3 times the interquartile range above the third quartile) were defined as lesions with mild or extreme high ^{18}F-DOPA uptake, respectively, and presence of these was determined in patients with 10 lesions or more.

Results: ^{18}F-DOPA was detected over 680 lesions in 38 patients, of which 35 were serotonin producing. ^{18}F-DOPA uptake varied with a median of 8-fold up to 44-fold between lesions within a patient. In 12 of 20 evaluable patients, lesions with mild high ^{18}F-DOPA uptake were found, and in 5, lesions with extreme high ^{18}F-DOPA uptake.

Conclusions: ^{18}F-DOPA-PET showed considerable heterogeneity in ^{18}F-DOPA uptake between tumor lesions and identified lesions within patients with mild or extreme high ^{18}F-DOPA uptake.

Key Words: ^{18}F-DOPA PET scan, heterogeneity, neuroendocrine tumor, tracer uptake

(*Clin Nucl Med* 2019;44: 612–619)

Neuroendocrine tumors of small intestine (SI-NETs) are rare tumors that in general are characterized by slow tumor growth. More than 50% of patients with NET present with metastatic disease. Symptoms are caused by tumor mass and/or (over)production of neuroendocrine amines such as serotonin.[1] Heterogeneity of tumor characteristics is increasingly appreciated and common in NETs and occurs at different genetic and epigenetic levels and in the expression of protein biomarkers.[2] In several pathology studies, heterogeneity between tumor lesions is shown. Immunohistochemical analysis of surgical specimens of liver metastases of 29 patients with pancreatic NET demonstrated heterogeneity within and between synchronous and metachronous metastases for Mindbomb E3 ubiquitin protein ligase 1, CD34, and somatostatin receptor 2 (SSTRA2).[3] In another study, in 14 of 27 patients with SI-NET, a discordant tumor grade between liver lesions was demonstrated.[4] This was also shown in pancreatic NETs, where 10 of 16 patients had a discordant tumor grade between nodal, liver, or other metastases.[5] Furthermore, 8 of 26 patients had tumor lesions with no to weak SSTRA2 expression and lesions with moderate to strong SSTRA2 expression.[6] For patients with SI-NET, a number of systemic and local treatment options are available. Selection of the most active tumor lesion for local treatment might be beneficial for patients with SI-NET to reduce symptoms caused by overproduction of neuroendocrine amines. Local treatment options consist of radiofrequency ablation, transarterial chemoembolization, transarterial embolization, resection, or the more recently developed selective internal radiation therapy (SIRT).[7,8] In patients with colorectal liver metastases, SIRT added to standard chemotherapy had a better median PFS in the liver than chemotherapy.[9] Currently, no studies analyzing heterogeneity between tumor lesions based on molecular imaging are available. In patients with SI-NET, the tumor can be visualized with several molecular imaging techniques. ^{18}F-DOPA visualizes the metabolism of catecholamine pathway in the tumor cell. Total tumor burden measured with ^{18}F-DOPA PET scans in patients with SI-NET correlates with tumor markers of the serotonin and catecholamine pathway.[10] We analyzed interlesional tumor ^{18}F-DOPA uptake heterogeneity with correction for background activity with PET scans and investigated if tumor lesions with substantially higher ^{18}F-DOPA uptake could be identified in patients with SI-NET.

MATERIALS AND METHODS

Patients

Patient records of all patients with NET undergoing an ^{18}F-DOPA PET scan at the University Medical Center of Groningen, the Netherlands, between February 2014 and April 2015, were screened. All adult patients with a metastasized SI-NET with visualization of more than 1 lesion on the ^{18}F-DOPA PET scan and who had undergone a diagnostic CT scan within 6 months of the PET scan were selected for further analysis (Fig. 1). The following baseline characteristics were retrospectively retrieved from patients' medical record: duration of disease, previous treatments, tumor grade (1 or 2) according to the 2010 World Health Organization classification, 5-HIAA level in 24-hour urine, and serotonin level in platelet-rich plasma. A tumor was considered serotonin-producing if either a 5-HIAA level in 24-hour urine greater than 3.8 mmol/mol creatinine or a serotonin level greater than 5.4 nmol/109 thrombocytes in platelet-rich plasma was measured.[11] ^{18}F-DOPA PET scans

Received for publication October 26, 2018; revision accepted April 11, 2019.
From the Departments of *Medical Oncology, †Radiology, and ‡Nuclear Medicine and Molecular Imaging, University of Groningen, University Medical Center Groningen, Groningen, the Netherlands.
Aline M. van der Loo–van der Schaaf is now with the Medical Center Zuiderzee, Lelystad, the Netherlands.
Conflicts of interest and sources of funding: none declared.
Correspondence to: Annemiek M. E. Walenkamp, MD, PhD, Department of Medical Oncology, University of Groningen, University Medical Center Groningen, DA11 PO Box 30.001, 9700 RB Groningen, the Netherlands. E-mail: a.walenkamp@umcg.nl.
Supplemental digital content is available for this article. Direct URL citation appears in the printed text and is provided in the HTML and PDF versions of this article on the journal's Web site (www.nuclearmed.com).

ISSN: 0363-9762/19/4408–0612
DOI: 10.1097/RLU.0000000000002640

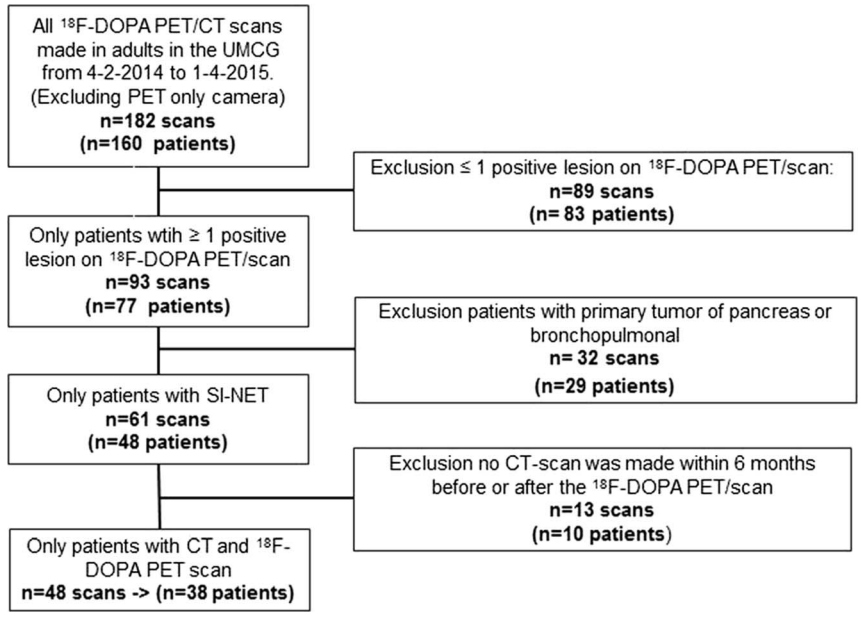

FIGURE 1. Flowchart of inclusion of ^{18}F-DOPA PET scans in interlesional heterogeneity study.

were conducted during standard care. Because of the retrospective nature of this analysis, according to the Dutch regulations and the ethical committee of our institution, no approval by this committee was needed, and no additional informed consent was required. The patient whose scan was used in Figure 3 gave informed consent for publication, according to author guidelines.

^{18}F-DOPA PET and CT Scan

^{18}F-DOPA was produced in the radiochemical laboratory of the University Medical Center of Groningen as described previously.[12] Patients fasted for 6 hours before the tracer injection and were allowed to continue all medications. For the reduction of tracer decarboxylation and subsequent renal clearance, all patients received 2 mg/kg carbidopa (maximum 150 mg) orally as pretreatment, 1 hour before the ^{18}F-DOPA injection to increase ^{18}F-DOPA uptake in tumor cells.[13] PET images were acquired 60 minutes after intravenous administration of ^{18}F-DOPA (170–215 MBq). Scanning was performed from the upper legs to head with a PET/CT camera (Siemens Biograph mCT 40 or 64 slices, 4 detector rings, Knoxville, TN) with zoom factor 1. Scanning time per bed position was 1 to 3 minutes, depending on body weight, and a low-dose CT was used for attenuation and scatter correction. PET data were reconstructed with Siemens Ultra HD (trueX and time of flight) and ordered subsets expectation maximization reconstruction, using 3 iterations and 21 subsets and a matrix of 400 with a full width at half maximum of 5-mm Gaussian (isotropic) filter.[10,14,15] The PET scan was combined, at the same time or within 6 months before or after date of PET scanning, with a contrast-enhanced diagnostic CT scan. A CT scan of the chest (n = 32) and abdomen (n = 38) was obtained, with iodine-containing intravenous, iomeprol (Iomeron) 350 mg/mL, and oral contrast agents. CT scans were performed on the Biograph mCT PET/CT, 40 slices or 64 slices; Somatom Sensation 64; or Somatom Definition Dual (all Siemens) with a maximal slice thickness of 2 mm.

Imaging Data Analysis

PET-positive tumor lesions were defined as lesions with an unequivocal visibility on ^{18}F-DOPA PET scan greater than normal activity in that body region.[16] Around all PET-positive tumor lesions, a volume of interest (VOI) was manually drawn on the PET scan with use of in-house–developed Accurate Software. In each "background organ," a spherical VOI was drawn in an area of homogenous activity in the organ, to quantify the physiological ^{18}F-DOPA uptake. The VOI diameter used to measure SUVmean in background organs was 1 cm in blood pool, bone marrow at L4 or L5, cortical bone of the humerus, and cortex of the kidney and pancreas; the VOI diameter was 2 cm in muscle, myocardium, and spleen; and the VOI diameter was 3 cm in brain, liver, and lung. SUVmax, SUVpeak, and SUVmean values were calculated according to the body weight of the patient.

To detect and quantify all tumor lesions, including PET-negative tumor lesions, ^{18}F-DOPA PET scans were compared with CT scans that were reviewed by a radiologist with knowledge of the PET data. The radiologist counted in each organ all abnormalities and defined these as definitely benign, definitely malignant, or as "inconclusive lesions." Afterward, all discrepancies between malignant lesions or inconclusive lesions on CT scan versus tumor lesions on ^{18}F-DOPA PET scans were reviewed by one of the investigators. If a PET-negative, definitely malignant or "inconclusive lesion" was found, a VOI was drawn surrounding the lesion on CT scan to calculate SUV values of the same region on the ^{18}F-DOPA PET scans. For small PET-negative lesions of less than 0.15 mL, like lung nodules, a spherical VOI with a diameter of 1 cm was drawn. In case of more than 20 liver lesions on ^{18}F-DOPA PET or CT scan, a cutoff of 20 lesions for both modalities was used. If more than 20 liver lesions were present, single lesions could not be identified separately and therefore could not be counted exactly. PET-negative, CT definitely malignant lesions were included for further analysis of ^{18}F-DOPA heterogeneity. Lesions that were "inconclusive" on CT and PET-negative were not used for further analysis of ^{18}F-DOPA heterogeneity. Heterogeneity was defined as ratio of uptake between lesion with the highest versus lesion with the lowest ^{18}F-DOPA uptake. Heterogeneity was compared between patients still alive at the moment of follow-up (April 2018).

Patients were evaluable for detection of lesions with mild or extreme high ^{18}F-DOPA uptake if more than 10 tumor lesions were

present, see for calculation below. ^{18}F-DOPA uptake in a tumor lesion was calculated by dividing the SUVpeak value of the tumor lesion by the SUVmean value measured in the VOI drawn in the background organ. To determine the "tumor burden" for each lesion or VOI, the uptake has to be multiplied by lesion or VOI volume.[10,17] This method was analyzed in a study using ^{18}F-FDG PET scans. SUVpeak corrected for local SUVmean background multiplied by volume had the most optimal feasibility and repeatability to measure metabolic active tumor volume (ie, tumor burden).[17] To explore the partial volume effect (PVE) of the results, SUVs of tumor lesions were correlated with tumor VOI volume, and the correlation was compared with the relation between SUV and volume seen in the NEMA NU 2-2007 phantom model.[18] To explore the effect of tissue density on SUV, the SUV of background organs was correlated with tissue density. Tissue density was based on the average Hounsfield units per VOI.

Statistical Analysis

Patients' demographic and clinical variables were summarized using medians with ranges for continuous variables and frequencies with percentages for categorical variables. The magnitude of heterogeneity between lesions within a patient was calculated by dividing the lesion with the highest ^{18}F-DOPA uptake with the lesion with the lowest ^{18}F-DOPA uptake within a patient. Differences between a median ^{18}F-DOPA uptake and SUVmean per organ were analyzed with the Kruskal-Wallis test. To determine lesions with mild or extreme higher ^{18}F-DOPA uptake than other lesions, the lower (Q1) and upper quartiles (Q3) were determined first. The interquartile range (IQR), or Q3–Q1, was then computed. Lastly, the upper fences were computed as follows: upper inner fence Q3 + 1.5 * (IQR) and upper outer fence Q3 + 3 * (IQR). Any data points outside the fences are considered as lesions with mild or extreme high ^{18}F-DOPA uptake, compared with the other lesions in that patient. Correlations of parametric values were calculated using Pearson *r*; nonparametric values were calculated using Spearman ρ. $P < 0.05$ was considered significant. Statistical analyses were performed using SPSS version 23 (SPSS, Inc, Chicago, Ill).

RESULTS

Patients

In the selected period, 182 ^{18}F-DOPA PET scans of 160 patients with SI-NET were obtained. Eighty-three patients were excluded because their scan showed no or only 1 tumor lesion, 29 patients had a primary NET of pancreatic or lung origin, and in 10 patients the time between ^{18}F-DOPA PET scan and CT scan was more than 6 months (Fig. 1). In total, 38 patients were eligible for analysis. Data of 5-HIAA urinalysis and serotonin in platelet-rich plasma were available for 34 and 38 patients, respectively. According to these data, 35 patients had a serotonin-producing NET. Baseline characteristics of included patients are shown in Table 1. Median age of the patients was 65 years (IQR, 55–70 years), and 55% of patients were male.

TABLE 1. Baseline Characteristics of SI-NET Patiens (n = 38)

Characteristic	No. Patients (%)
Sex (male)	21 (55)
Tumor grade	
1	27 (71)
2	3 (8)
Unknown	8 (21)
Treatment	
SSA use	23 (61)
Surgery	22 (58)
Everolimus	1 (3)
Interferon	3 (8)
PRRT	1 (3)
Any treatment	26 (68)
Patients with serotonin-producing tumor	35 (92)

PRRT indicates peptide radionuclide receptor therapy.

Analysis of Tumor Lesions Measured With ^{18}F-DOPA PET

More than 680 tumor lesions were visualized on the ^{18}F-DOPA PET scans (mean, >20 lesions per patient). The median SUVpeak in tumor lesions was 5.5 (IQR, 3.1–11.2), and the median ^{18}F-DOPA uptake was 4.1 (IQR, 2.2–7.7). In total, 581 ^{18}F-DOPA PET lesions could be correlated to a morphologic lesion on CT scan (Supplemental data Fig. S1, Supplemental Digital Content 1, http://links.lww.com/CNM/A195). Thirty-eight ^{18}F-DOPA PET–negative lesions were detected by CT scan. In 1 patient, the CT scan revealed 2 liver metastases that were not detected on ^{18}F-DOPA PET scan, and these were included for analysis of ^{18}F-DOPA heterogeneity. Of 36 other ^{18}F-DOPA PET–negative lesions detected by CT scan, mostly localized in lung and lymph nodes, no differentiation could be made on CT whether the lesions were benign or malignant, and these were not analyzed. In some patients, 1 PET lesion referred to 2 or more CT lesions, because the lesions were merged with each other on ^{18}F-DOPA PET scan. Seven lesions were seen on the PET scan but outside the field of view on CT scan.

Examination of the lesions per organ showed 91 bone lesions visible on ^{18}F-DOPA PET scan, inside the view of field of the CT scan, but not visible on CT scan. When we evaluated other organs than the skeleton, a small number of lesions were revealed only on ^{18}F-DOPA PET scan (liver, lymph node/mesenterium, lung) or only on CT scan (lung) (Supplemental data Fig. S1, Supplemental Digital Content 1, http://links.lww.com/CNM/A195).

Interlesional Heterogeneity and Physiological ^{18}F-DOPA Uptake

The ^{18}F-DOPA uptake ranged from 1- to 44-fold between individual lesions within the same patient (median, 8-fold) (Table 2). Twelve of the 20 patients with more than 10 tumor lesions had lesions with mild high ^{18}F-DOPA uptake, and 5 patients had lesions with extreme high ^{18}F-DOPA uptake (Figs. 2, 3). Liver, lymph nodes combined with mesenterium, bone, and lungs were most frequently involved. Tumor burden per lesion is depicted in the Supplemental Figure S2 (Supplemental Digital Content 2, http://links.lww.com/CNM/A196). The median ^{18}F-DOPA uptake of all analyzed lesions differed per organ ($P < 0.05$) (Fig. 4). Lesions in the lung had the highest ^{18}F-DOPA uptake (median, 8.4), and lesions of the heart the lowest (median, 1.7).

The median of SUVmean values measured in the background organs of all patients was 1.2 (IQR, 0.9–1.5) and differed per organ ($P < 0.05$) (Fig. 5, Table 3).

Thirty-one patients were still alive at the moment of the last follow up (April 2018). Mean ^{18}F-DOPA uptake ranged from 1- to 44-fold between individual lesions within the same patient (median, 8-fold). Seven patients died; their mean ^{18}F-DOPA uptake ranged from 4- to 25-fold between individual lesions within the same patient (median, 8-fold).

TABLE 2. Tracer Uptake, Magnitude of Heterogeneity and Number of Lesions With Mild or Extreme High Tracer Uptake

Characteristics of Metastases			Tracer Uptake			
Patient	Lesions, n	Metastasized Organs	Mean	Max vs Min	MH,* n	EH,* n
1	>65	Lung, liver, pancreas, LN, bone, other	6.5	43.6	3	1
2	17	Liver	2.2	3.7	0	0
3	3	Liver, LN	1.5	1.2	—	—
4	38	Lung, liver, LN	6.0	3.6	0	0
5	6	Bowel, LN	3.0	3.0	—	—
6	5	Lung, Liver	3.4	1.8	—	—
7	>32	Liver, LN	6.6	9.5	0	0
8	9	Liver, pancreas, bowel, LN, other	3.3	5.3	—	—
9	14	Liver	3.9	8.5	1	0
10	13	Lung, liver, LN	7.0	22.1	0	0
11	17	Liver, bowel, LN	2.7	5.6	2	1
12	5	LN	8.1	15.0	—	—
13	7	Heart, pancreas, bowel, LN, other	5.7	6.2	—	—
14	9	Liver, LN	2.5	2.2	—	—
15	38	Lung, liver, LN, bone, Other	12.4	42.3	2	0
16	12	Lung, pancreas, LN, bone	6.1	3.8	0	0
17	2	Bowel, LN	9.5	12.5	—	—
18	>40	Liver, bowel, LN, bone, other	7.5	30.7	3	1
19	9	Liver, bowel, LN	10.6	28.7	—	—
20	6	LN, bone	13.7	28.0	—	—
21	5	Liver, LN	3.5	8.4	—	—
22	4	Pancreas, LN	10.5	8.3	—	—
23	46	Liver, pancreas, LN, bone	7.8	25.0	1	0
24	17	Liver, LN	3.8	8.6	1	0
25	13	Liver, pancreas, other	3.5	5.0	0	0
26	20	Liver, pancreas, LN, bone	5.3	10.9	0	0
27	>30	Heart, liver, LN, bone, other	7.7	13.9	4	0
28	>23	Liver, LN	5.8	11.2	0	0
29	4	Bowel, LN	5.2	2.9	—	—
30	7	Liver	1.6	1.4	—	—
31	3	LN	2.8	2.1	—	—
32	5	LN	4.0	2.1	—	—
33	>54	Lung, liver, LN, bone, other	10.3	171	3	0
34	5	Heart, bowel, LN	5.5	6.2	—	—
35	15	Liver, LN	3.1	6.5	1	0
36	8	Liver, bowel, LN	4.0	9.1	—	—
37	15	Liver, bone	6.2	17.2	1	1
38	>48	Liver, LN, bone, other	2.8	8.4	9	7

EH indicates lesion with extreme higher ^{18}F-DOPA uptake than other lesions; LN, lymph node; Max vs min, lesion with the highest tracer uptake divided by lesion with the lowest tracer uptake within a patient; MH, lesion with mild higher ^{18}F-DOPA uptake than other lesions.

*Lesions with mild or extreme high ^{18}F-DOPA uptake compared with other lesions were determined only if more than 10 lesions were present.

Effect of Partial Volume Effect and Tissue Density on Physiological ^{18}F-DOPA Uptake

SUVpeak and ^{18}F-DOPA uptake of all tumor lesions were correlated with their volumes, $r = 0.20$ ($P = 7.33 * 10^{-8}$) and $r = 0.15$ ($P = 6.7 * 10^{-5}$), respectively (Fig. 6). SUVmean of healthy lung was linearly correlated with tissue density $r = 0.83$ ($P = 1.28 * 10^{-10}$) (Fig. 7, Table 3).

DISCUSSION

^{18}F-DOPA PET scans showed interlesional tumor heterogeneity within patients with SI-NET and identified lesions with mild or extreme high ^{18}F-DOPA uptake in 60% of the evaluable patients.

Interlesional tumor heterogeneity of NET tumor characteristics within patients has been shown in several pathology studies.[4–6,19] We are not aware of currently performed studies that aim to identify tumor lesions with higher ^{18}F-DOPA uptake in patients with SI-NET lesions. We performed refined analyses of tumor burden with the use of tumor-to-background ratio to compensate for differences between organs in tracer uptake, vessel density, and permeability.[17,20] With the knowledge that interlesional tumor heterogeneity in NETs can be determined with ^{18}F-DOPA PET, we were interested if lesions with mild or extreme high ^{18}F-DOPA uptake could be identified.

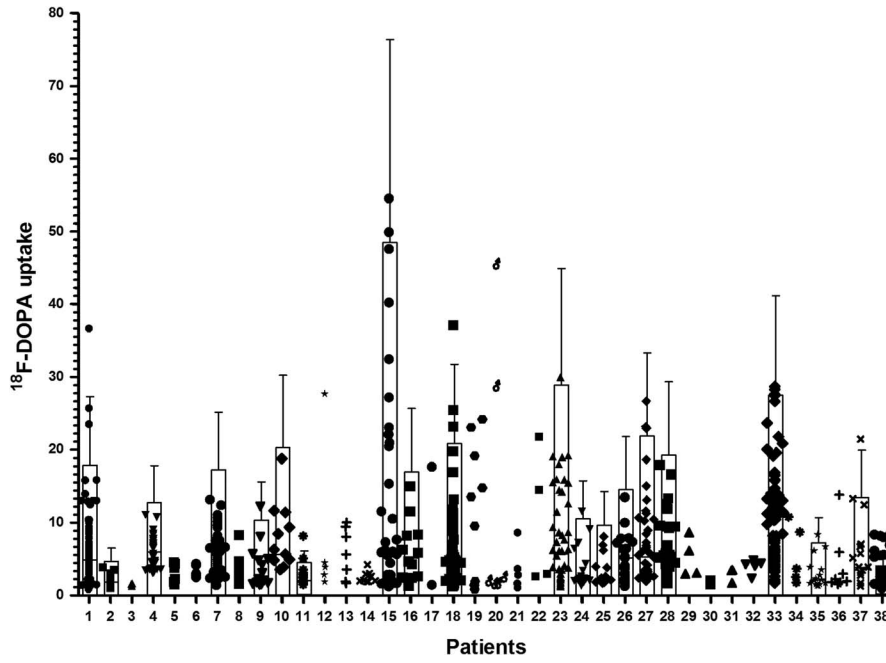

FIGURE 2. ^{18}F-DOPA uptake per tumor lesion per patient. Tumor lesions above the inner and outer upper fences show mild or extreme high ^{18}F-DOPA uptake in patients with 10 tumor lesions or more. Each symbol represents a single lesion. Color and kind of symbol are equal per lesion within a patient.

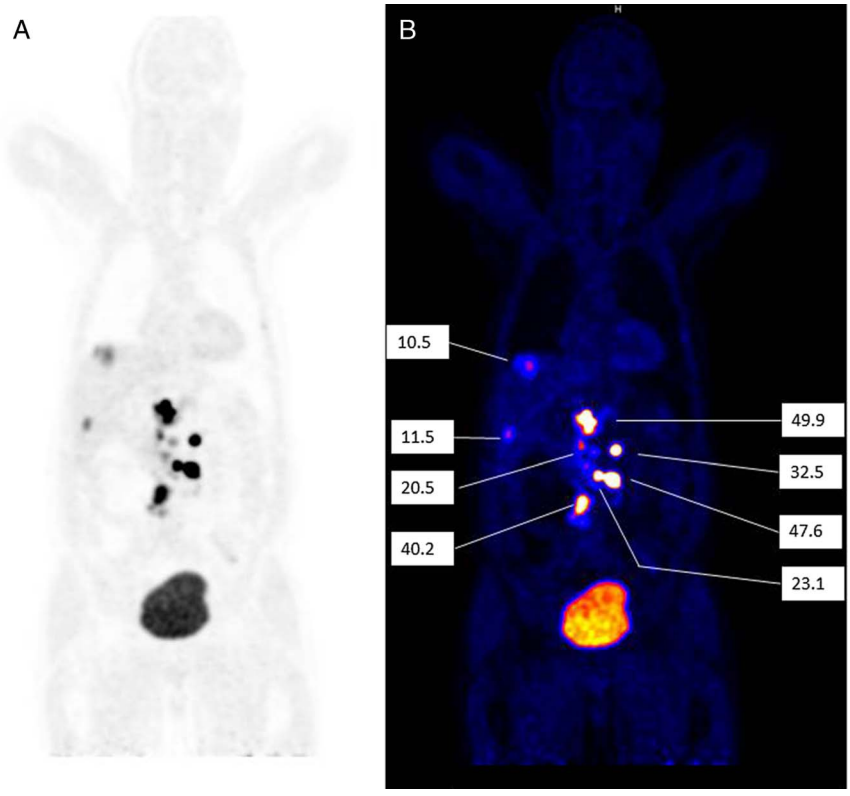

FIGURE 3. Representative ^{18}F-DOPA PET scan. ^{18}F-DOPA uptake per lesion in patient 15. **A**, ^{18}F-DOPA PET scan. **B**, ^{18}F-DOPA PET scan fused with low-dose CT scan. Written informed consent for publication of the clinical images was obtained from the patient.

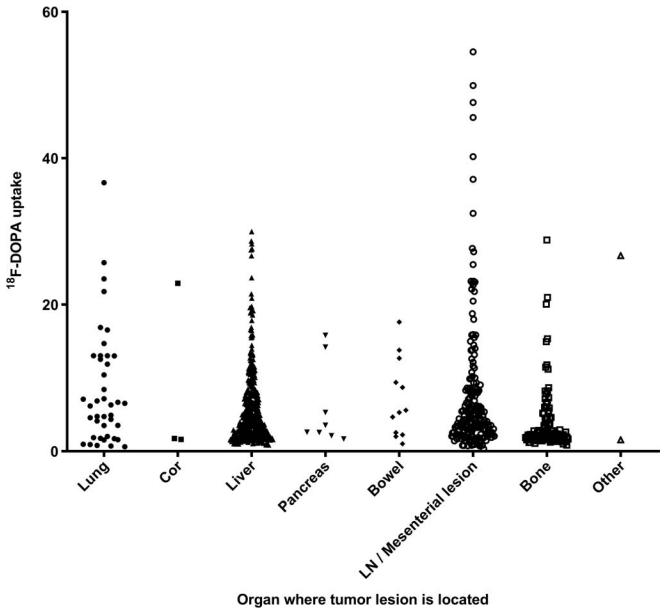

FIGURE 4. ^{18}F-DOPA uptake per tumor lesion according to location in the body. SUVpeak per tumor VOI according to location. Each symbol represents a single lesion. Kind of symbol is equal per lesion in the same kind of organ. LN indicates lymph node.

Because total tumor burden measured on ^{18}F-DOPA PET correlates with 5-HIAA in urine, a better insight in heterogeneity could potentially be used in case of systemic symptoms.[9] In patients with symptomatic liver metastases, local treatments with radiofrequency ablation, transarterial chemoembolization, transarterial embolization, resection, or SIRT are relevant treatment modalities.[9] With the selection of tumor lesions with a relatively high tumor burden, local treatments might be more effective in symptom management than selection based on other characteristics. In general, tumor heterogeneity in neoplasms is determined by genetic variation between subclones of tumor cells. As a consequence, cell clones that have an advantage within a given tumor microenvironmental context survive and can expand through Darwinian selection.[2] This may lead to tumor adaptation and therapeutic failure.[21] Interlesional tumor heterogeneity on ^{18}F-DOPA PET was rudimentarily analyzed in an imaging study in 77 NET patients. The SUVmax, without correction for the SUV of the background organ, between lesions within the patient, varied up to 29-fold.[10] In NETs, a study analyzed heterogeneity within a single tumor lesion. One hundred forty-one NET patients, of which 108 patients had a gastroenteropancreatic NET, underwent a ^{68}Ga–somatostatin analog (SSA) PET scan to select them for radiolabeled peptide receptor therapy. Heterogeneity within a lesion was shown to be present, and entropy (a heterogeneity parameter) appeared to be predictive for progression-free survival and overall survival.[22] In our data set, no relation between interlesional tumor heterogeneity and survival could be shown.

Recently, it was shown that total tumor burden in patients with SI-NET measured with ^{68}Ga-SSA PET scan correlated with tumor markers, with 5-HIAA level in 24-hour urine and with chromogranin A; however, this study did not investigate heterogeneity between tumor lesions.[23] In another study, in 5 patients the genetic heterogeneity between primary and metastatic lesions was evaluated by whole-exome sequencing. This revealed a highly varying degree of genetic heterogeneity between primary lesions and hepatic metastasis.[24]

In studies where sensitive molecular scans are used like in this study, many small tumor lesions could become visible. In small lesions, the PVE has to be taken into account. Part of variability in SUV might be explained by the PVE. This is demonstrated in the nonlinear curve of our data, similar to the curve derived from the phantom model (Fig. 6).[25,26] In total, 90% of lesions in our study were smaller than 20 mL, and therefore their SUVs could be influenced by PVEs.

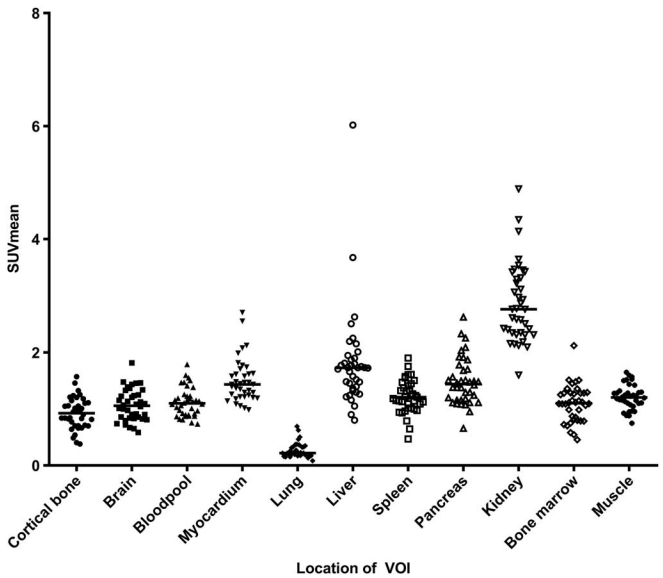

FIGURE 5. SUVmean per VOI according to location in the body of nontumoral tissue. The VOIs per organ were of the same size per organ. The bar is showing the median. Each symbol represents a single VOI. Kind of symbol is equal per VOI in the same kind of organ.

TABLE 3. Median SUVmean Value of Each Background Organ and Correlation With Tissue Density

Organ	SUVmean, Median (Range)	Correlation SUVmean With Tissue Density (Pearson *r*)	*P*
Kidney	2.8 (2.3–3.3)	0.04	NS
Liver	1.7 (1.3–1.9)	0.01	NS
Pancreas	1.5 (1.2–1.7)	−0.09	NS
Myocardium	1.4 (1.2–1.6)	−0.11	NS
Spleen	1.2 (1.0–1.4)	−0.16	NS
Muscle	1.2 (1.1–1.3)	−0.09	NS
Bone marrow	1.1 (0.8–1.3)	0.10	NS
Blood pool	1.1 (0.9–1.2)	0.00	NS
Brain	1.1 (0.8–1.3)	0.07	NS
Cortical bone	0.9 (0.7–1.1)	−0.17	NS
Lung	0.2 (0.2–0.3)	0.83	$1.28 * 10^{-10}$
Total	1.2 (0.9–1.5)	0.22	$5 * 10^{-6}$

NS indicates not significant.

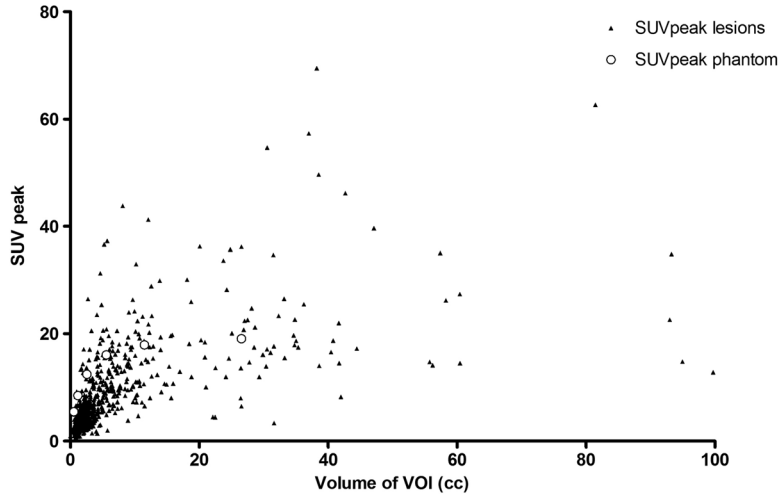

FIGURE 6. Partial volume effect compared with a phantom model. SUVpeak of the lesion versus the volume of the lesion, compared with the curve of the PVE measured with a phantom.

A component of PVE is tissue fraction effect (TFE).[27] Healthy lung tissue has a lower density because it contains air. It is found that an increase in observed SUV is associated with regions of increased lung density.[27,28] In our analysis, this is reflected in a linear correlation between lung density with the SUV and a lower SUVmean of lung tissue compared with SUVmean value of the other organs used for background measurement (Fig. 7). This resulted in higher ^{18}F-DOPA uptake in lung lesions compared with lesions in other organs (Fig. 4). Several methods are developed to correct for TFE in lung.[27,28] In follow-up studies, to select lesions with substantially higher ^{18}F-DOPA uptake for local treatment, the TFE and PVE have to be taken into account.

CONCLUSIONS

In patients with SI-NET, ^{18}F-DOPA uptake shows considerable heterogeneity in uptake between tumor lesions within a patient. Furthermore, in some patients, lesions with mild or extreme high ^{18}F-DOPA uptake could be identified. This suggests that ^{18}F-DOPA PET scans can serve, in patients with systemic symptoms,

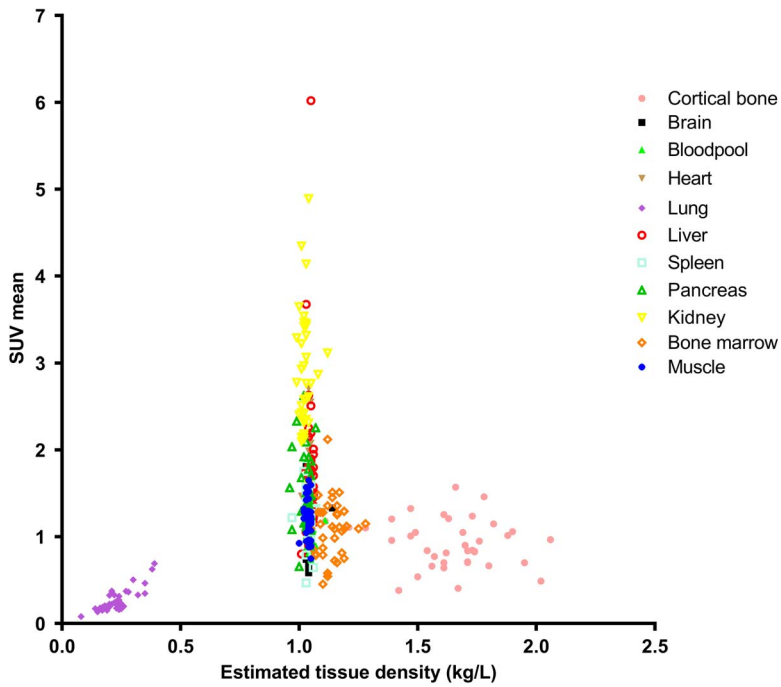

FIGURE 7. SUVmean per VOI according to tissue density.

due to an overproduction of catecholamines, to select lesions with substantially higher ^{18}F-DOPA uptake for local treatment.

REFERENCES

1. Raut CP, Kulke MH, Glickman JN, et al. Carcinoid tumors. *Curr Probl Surg*. 2006;43:383–450.
2. Burrell RA, McGranahan N, Bartek J, et al. The causes and consequences of genetic heterogeneity in cancer evolution. *Nature*. 2013;501:338–345.
3. Couvelard A, Deschamps L, Ravaud P, et al. Heterogeneity of tumor prognostic markers: a reproducibility study applied to liver metastases of pancreatic endocrine tumors. *Mod Pathol*. 2009;22:273–281.
4. Shi C, Gonzalez RS, Zhao Z, et al. Liver metastases of small intestine neuroendocrine tumors: Ki-67 heterogeneity and World Health Organization grade discordance with primary tumors. *Am J Clin Pathol*. 2015;143:398–404.
5. Richards-Taylor S, Tilley C, Jaynes E, et al. Clinically significant differences in Ki-67 proliferation index between primary and metastases in resected pancreatic neuroendocrine tumors. *Pancreas*. 2017;46:1354–1358.
6. Charoenpitakchai M, Liu E, Zhao Z, et al. In liver metastases from small intestinal neuroendocrine tumors, SSTR2A expression is heterogeneous. *Virchows Arch*. 2017;470:545–552.
7. Pavel M, Baudin E, Couvelard A, et al. ENETS Consensus Guidelines for the management of patients with liver and other distant metastases from neuroendocrine neoplasms of foregut, midgut, hindgut, and unknown primary. *Neuroendocrinology*. 2012;95:157–176.
8. Kennedy A, Bester L, Salem R, et al. Role of hepatic intra-arterial therapies in metastatic neuroendocrine tumours (NET): guidelines from the NET-Liver-Metastases Consensus Conference. *HPB*. 2015;17:29–37.
9. van Hazel GA, Heinemann V, Sharma NK, et al. SIRFLOX: randomized phase III trial comparing first-line mFOLFOX6 (plus or minus bevacizumab) versus mFOLFOX6 (plus or minus bevacizumab) plus selective internal radiation therapy in patients with metastatic colorectal cancer. *J Clin Oncol*. 2016;34:1723–1731.
10. Fiebrich HB, de Jong JR, Kema IP, et al. Total ^{18}F-DOPA PET tumour uptake reflects metabolic endocrine tumour activity in patients with a carcinoid tumour. *Eur J Nucl Med Mol Imaging*. 2011;38:1854–1861.
11. Kema IP, de Vries EG, Schellings AM, et al. Improved diagnosis of carcinoid tumors by measurement of platelet serotonin. *Clin Chem*. 1992;38:534–540.
12. Luurtsema G, Boersma HH, Schepers M, et al. Improved GMP-compliant multi-dose production and quality control of 6-[^{18}F]fluoro-L-DOPA. *EJNMMI RadiopharmChem*. 2017;1:7.
13. Koopmans KP, de Vries EG, Kema IP, et al. Staging of carcinoid tumours with ^{18}F-DOPA PET: a prospective, diagnostic accuracy study. *Lancet Oncol*. 2006;7:728–734.
14. Hudson HM, Larkin RS. Accelerated image reconstruction using ordered subsets of projection data. *IEEE Trans Med Imaging*. 1994;13:601–609.
15. van Asselt SJ, Oosting SF, Brouwers AH, et al. Everolimus reduces ^{89}Zr-bevacizumab tumor uptake in patients with neuroendocrine tumors. *J NuclMed*. 2014;55:1087–1092.
16. Koopmans KP, Neels OC, Kema IP, et al. Improved staging of patients with carcinoid and islet cell tumors with ^{18}F-dihydroxy-phenyl-alanine and ^{11}C-5-hydroxy-tryptophan positron emission tomography. *J Clin Oncol*. 2008;26:1489–1495.
17. Frings V, van Velden FH, Velasquez LM, et al. Repeatability of metabolically active tumor volume measurements with FDG PET/CT in advanced gastrointestinal malignancies: a multicenter study. *Radiology*. 2014;273:539–548.
18. National Electrical Manufacturers Association. NEMA Standards Publication NU 2-2007, Performance Measurements of Positron Emission Tomographs. Rosslyn, VA: NEMA; 2007.
19. Francis JM, Kiezun A, Ramos AH, et al. Somatic mutation of CDKN1B in small intestine neuroendocrine tumors. *Nat Genet*. 2013;45:1483–1486.
20. Bol K, Haeck JC, Groen HC, et al. Can DCE-MRI explain the heterogeneity in radiopeptide uptake imaged by SPECT in a pancreatic neuroendocrine tumor model? *PloS One*. 2013;8:e77076.
21. Gerlinger M, Rowan AJ, Horswell S, et al. Intratumor heterogeneity and branched evolution revealed by multiregion sequencing. *N Engl J Med*. 2012;366:883–892.
22. Werner RA, Lapa C, Ilhan H, et al. Survival prediction in patients undergoing radionuclide therapy based on intratumoral somatostatin-receptor heterogeneity. *Oncotarget*. 2017;8:7039–7049.
23. Tirosh A, Papadakis GZ, Millo C, et al. Association between neuroendocrine tumors biomarkers and primary tumor site and disease type based on total (68)Ga-DOTATATE–avid tumor volume measurements. *Eur J Endocrinol*. 2017;176:575–582.
24. Walter D, Harter PN, Battke F, et al. Genetic heterogeneity of primary lesion and metastasis in small intestine neuroendocrine tumors. *Sci Rep*. 2018;8:3811–018-22115-0.
25. Hoetjes NJ, van Velden FH, Hoekstra OS, et al. Partial volume correction strategies for quantitative FDG PET in oncology. *Eur J Nucl Med Mol Imaging*. 2010;37:1679–1687.
26. Hoffman EJ, Huang SC, Phelps ME. Quantitation in positron emission computed tomography: 1. Effect of object size. *J Comput Assist Tomogr*. 1979;3:299–308.
27. Holman BF, Cuplov V, Millner L, et al. Improved correction for the tissue fraction effect in lung PET/CT imaging. *Phys Med Biol*. 2015;60:7387–7402.
28. Lambrou T, Groves AM, Erlandsson K, et al. The importance of correction for tissue fraction effects in lung PET: preliminary findings. *Eur J Nucl Med Mol Imaging*. 2011;38:2238–2246.